SPE 151879

Determination of Saturation Distributions in Water Displacement by Analytical Models

S. Alireza Haghighat, Shahab D. Mohaghegh, West Virginia University

This paper was prepared for presentation at the North Africa Technical Conference and Exhibition held in Cairo, Egypt, 20–22 February 2012.

Abstract

Water is injected in the hydrocarbon reservoir to serve two purposes, to maintain reservoir pressure and to displace oil as production proceeds in the reservoir.

In recent years, smart wells coupled with reservoir simulation models are used to improve the results of water injection performance. High frequency data (pressure, flow rate, etc.) that is a product of the smart wells provide the basis for a closed-loop, fast track updating of the dynamic reservoir models. While high frequency updating of the reservoir model remains a challenge, there are emerging technologies that can make such objectives achievable. An integrated approach that combines analytical and numerical solutions with artificial intelligence and data mining is proposed to ultimately achieve the closed-loop, fast track updating system. This study is the first step in that direction.

In this work the ability of analytical solutions to calculate reservoir water saturation profiles from field water cut data are investigated. Different flow regimes and reservoir geometries are considered during this study. Diffuse, segregated and capillary influenced flow models are analyzed in both one and two dimensional water injection using a commercial numerical simulator.

Different analytical formulations are applied for each flow regime in order to reproduce simulation production data. For each model a specific relative permeability relation is assigned and tuned with the aim of matching water breakthrough time and water cut history. An accurate match is achieved between water saturation profiles generated by the analytical models and the results by the reservoir simulator. The influence of simple reservoir heterogeneity on the robustness of the analytical models is studied.

Introduction

In the past 2 decades, permanent down-hole gauges have been used widely in the petroleum industry for continuous monitoring of pressure, flow rates and automatic flow controls. The advancement of in-situ reservoir measurement and monitoring system introduced the concept of “Smart Field “in the oil and gas industry. The objective of the “Smart Field” technology is summarized in optimization of the reservoir performance by real-time decision making based on the integration of high frequency measurements and the reservoir model. Generally, sophisticated numerical reservoir simulations with complex computations and a noticeable high run time are mainly used for reservoir modeling in oil industry. Making real time reservoir management decision based on online data from the field requires a substitute for the sophisticated numerical reservoir models which are able to predict the reservoir performance in a shorter run time.

Analytical, low-ordered and proxy models, in addition to CRM (Capacitance-Resistive Model[10]) or SRM (Surrogate Reservoir Model[8]), can be considered as an alternative for numerical simulator models in the Closed-Loop Reservoir management work flow. This study aims to investigate the efficacy of analytical models in order to predict reservoir fluid distribution under water displacement.

Water flooding is considered the most commonly applied method of the secondary oil recovery process (Ahmed[1]). During water flooding, the fluid flow condition in the reservoir can be classified in piston-like (or diffuse), segregated and capillary influenced flow according to the injection rate and relative amount of reservoir thickness to the capillary transition zone length (Dake[4]). Buckley and Leverett’s theory has been widely used to describe fluid flow and displacement efficiency analytically during immiscible flooding. For high injection rates and low h (reservoir thickness) to H (capillary transition zone thickness) ratio, the flow is called piston-liked. Since the oil and water can be assumed to be incompressible this theory is applied to determine the fraction of oil and water in the produced fluids.

Relative permeability and, more specifically, fractional flow curves seem to be the most important source of information for describing reservoir performance and particularly water production trends during water displacement. Since the fractional flow curves are a function of fluid saturation, production data specially water cut can represent fluid distribution in the reservoir. As a result it is possible to determine reservoir water saturation based on production data.

Detrich[5] *et al* (1975) presented a trial and error graphical procedure based on fractional flow equations and production data to determine reservoir fluid saturation. This method provides fluid saturation in the vicinity of wells by use of the core relative permability curves. Ershaghi[6] *et al* (1978) proposed a technique for obtaining the fractional flow curves based on the water cut data. Their work was limited to reservoirs that produce with water cuts higher than 50%. Kulkarini[7] *et al* (2000) used the streamline approach to determine relative permeability curves. Their method provides a fast (single run) answer (none uniqueness) for relative permeability determination. Sitros[9] *et al* (2006) developed *fw* (water cut) versus *Sw* for horizontal wells using production data, material balance and the Corey equation.
In this study we consider a simple reservoir undergoing water flooding. We determine the water saturation profile (vs. time) at each location based on the Buckley- Leverett and Deits-Dupuit's[2] formulation. Water saturation at the production well location is used to determine the water cut history. For each formulation (Buckley-Leverett, Deits-Dupuit) the fractional flow curve is modified to generate the same water cut history as the simulation output. The history matched fractional flow curve (relative permeability) can replicate the simulated saturation profiles.

Methodology

In general the saturation profile by the Buckley-Leverett's formulation consists of three parts: rarefaction, front (shock) and constant saturation (**Fig. 1**). This saturation profile is determined by the fractional flow curve which describes the ratio of flowing water to the total flow in the reservoir as *eq. 1*(capillary and gravity forces are disregarded).

$$f_w = \frac{q_w}{q_o+q_w} = \frac{1}{1+\frac{\mu_w}{\mu_o}\frac{k_{ro}}{k_{rw}}} \qquad (eq.1)$$

Welge's (1952) method proposed drawing a tangent line to fractional flow curves (as a function of saturation) from ($S_{wc}, f_w = 0$). So the saturation at the front (S_{wf}) is obtained at the point of tangency (**Fig. 2**).

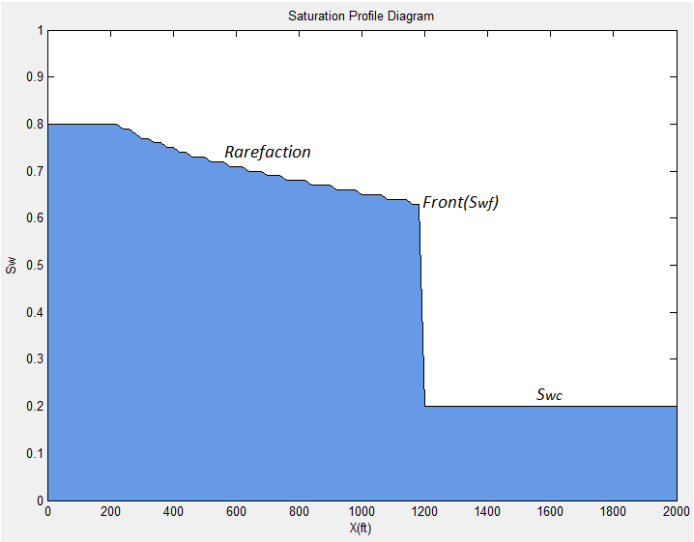

Fig. 1-Water saturation profile as function of distance

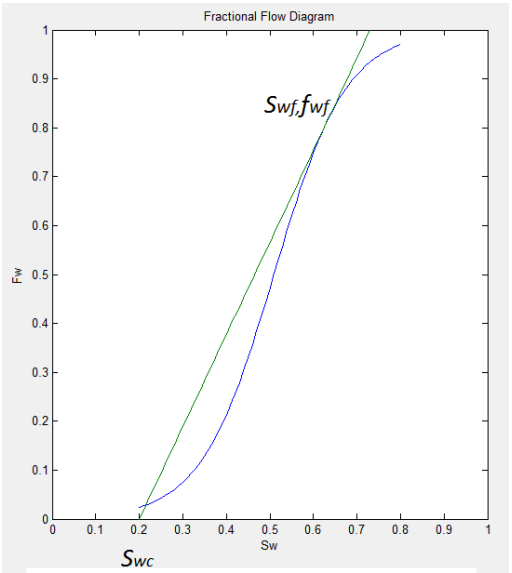

Fig. 2-Determination of front saturation

The velocity of the water front is proportional to the derivative of the fractional flow with respect to saturation; thus at any given time the position of front is related to cumulative water injection of W_i by:

$$X_{S_{wf}} = \frac{W_i}{\varphi A} \times \left(\frac{df_w}{dS_w}\right)_{S_{wf}} \qquad (eq.2)$$

To construct the rarefaction part ($X < X_{S_{wf}}$), the derivative of the fractional flow with respect to water saturation should be determined from *eq.2* at any position. The corresponding S_w (can be found graphically or by *eq.6*) from any calculated $\frac{df_w}{dS_w}$ is the water saturation at each point. After water breakthrough, $\frac{df_w}{dS_w}$ at the production well for any point in time can be calculated from *eq.2* knowing $X = L$ (distance between injection and production wells). The corresponding S_w for the calculated derivative is water saturation at well. S_w at the well location leads to determination of well water cut considering the formation volume factors of the oil and water (*eq.*3):

$$f_{ws} = \frac{1}{1+\frac{B_w}{B_o}(\frac{1}{f_w}-1)} \qquad (eq.3)$$

To address the fractional flow curve and its derivatives as the function of saturation, the relative permeability ratio is arrived at through the following exponential from:

$$\frac{K_{ro}}{K_{rw}} = ae^{bS_w} \qquad (eq.4)$$

By substituting the above equation in the fractional flow relation (*eq.1*), f_w and its derivative as the function of water saturation is obtained:

$$f_w = \frac{1}{1 + \left(\frac{\mu_w}{\mu_o}\right) abe^{bS_w}} \qquad (eq.5)$$

$$\left(\frac{df_w}{dS_w}\right) = \frac{-(\frac{\mu_w}{\mu_o})abe^{bS_w}}{[1 + \left(\frac{\mu_w}{\mu_o}\right) abe^{bS_w}]^2} \qquad (eq.6)$$

A reservoir simulation model for water flooding in a one-dimensional model is considered in this study. Since it is assumed that relative permeability and consequently fractional flow curves are unknown for the analytical model, "a" and "b" should be determined in a way that the difference between simulation and analytical water cut history is minimized. When "a" and "b" are found, consequently analytical water saturation distribution is matched with simulation results.

For the segregated flow (**Fig. 3,** top) the movement of water can be regarded stable if $G > M - 1; M > 1$ where G is gravity number ($\frac{k\acute{k}_{r_w} A\Delta\rho g \sin\theta}{1.013\times10^6 q_t \mu_w}$) and M is end point mobility ratio ($\frac{\acute{k}_{rw}}{\mu_w} / \frac{\acute{k}_{ro}}{\mu_o}$). Under this condition the angle (β) between the fluids interface and the direction of flow remains constant and is determined by *eq.7*.

$$-\tan\beta = \left(\frac{M - 1 - G}{G}\right)\tan\theta \qquad (eq.7)$$

This angle determines the fractional thickness (b_f) of the water at each location and the front speed ($v = \frac{qt}{\varphi A(1-S_{wc}-S_{or})}$) specifies the location of the water front at each time. Based on the value of fractional water thickness and the fact that water saturation in the water and oil phase is respectively $1 - S_{o_r}$ and S_{w_c}, the average water saturation at any distance is defined by (eq.8):

$$S_w = b_f(1 - S_{o_r}) + (1 - b_f)S_{wc} \qquad (eq.8)$$

After water breakthrough, the water saturation at the well can be determined based on the fractional water thickness and then consequently the production water cut is found by *eq.3*. It should be mentioned that for the segregated flow, relative permeability is a linear function of thickness averaged water saturation (Dake[4]). Therefore only end point relative permeability ($\acute{k}_{r_o}$ and $\acute{k}_{r_w}$) are considered as tuning parameters to match analytical results with simulation water cuts. In the case that the water interface is not stationary($G < M - 1$, **Fig. 3** bottom), the position of the fractional water thickness is computed by the (eq.9):

$$X_{b_f} = \frac{W_i}{A\varphi(1 - S_{wc} - S_{or})} \times \frac{M(b_f{}^2 G + 1) - (b_f - 1)^2 G}{(Mb_f + (1 - b_f))^2} \qquad (eq.9)$$

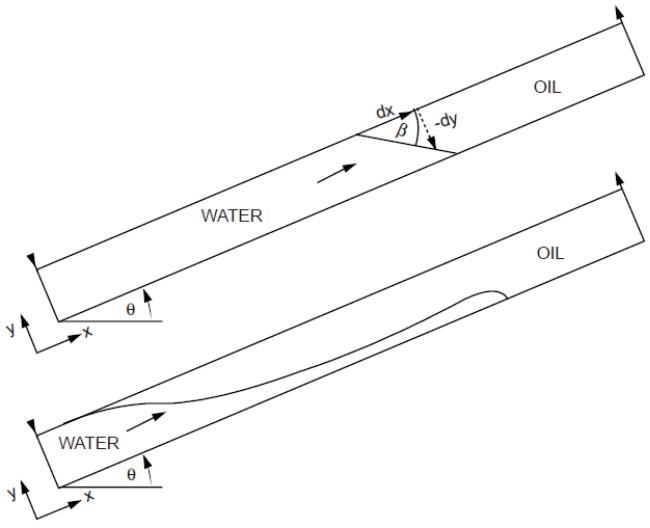

Fig. 3-Segregated flow with stable (top) and unstable (bottom) interface (Dake[4])

For the capillary influenced flow ($h_{res} = H_{capillary}$) pseudo relative permeability curves (Corey type relative permeability function) are considered to describe the water displacement as follow:

$$k_{r_w} = \acute{k}_{r_w}\left[\frac{S_w - S_{w_c}}{1 - S_{w_c} - S_{o_r}}\right]^{n_w} \qquad (eq.10)$$

$$k_{r_o} = \acute{k}_{r_o}\left[\frac{1 - S_w - S_{o_r}}{1 - S_{w_c} - S_{o_r}}\right]^{n_o} \qquad (eq.11)$$

In this type of flow, Buckley-Leverett's formulation and Welge's method are applied. Corey coefficients (n_w , n_o) are considered as the matching parameter for matching analytical results with simulation water cuts.

Base Models

In this work piston-like, segregated and capillary influenced water flooding is considered for one dimensional homogenous reservoir. Also piston-like flow was studied for one dimensional-heterogeneous and two dimensional homogenous models.

For the piston-like flow, the reservoir (**Fig. 4**) is discretized into $25 \times 1 \times 1$ grid blocks (dimension of each block is $80 \times 300 \times 10\ ft$). The water is injected in the first grid and oil is produced from the last grid (25^{th}). Since the fluids are considered to be incompressible, injection and production rates are equal. Relative permeability, capillary pressure and reservoir properties are shown in **Figs 5**, **Fig. 6** and **Table 1**.

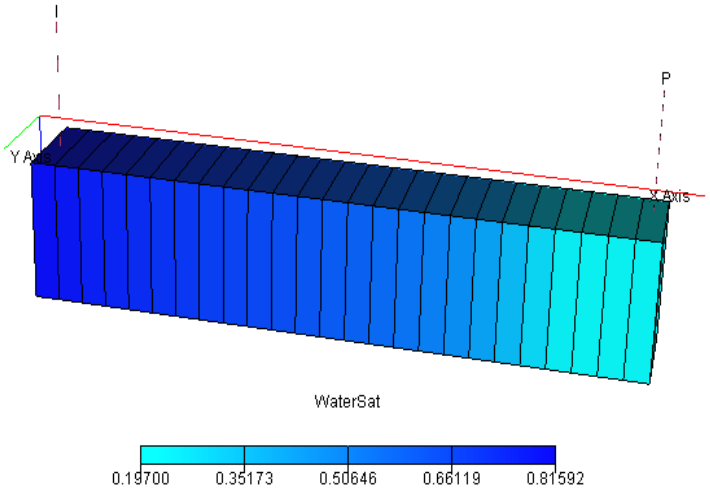

Fig. 4-Water saturation distribution for piston-like flow

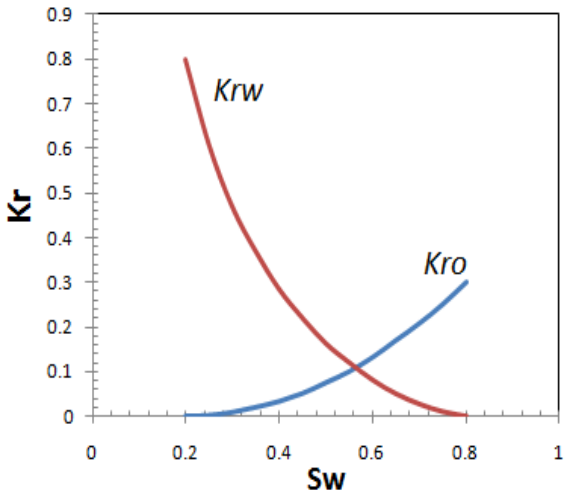

Fig. 5-Relative permeability curves for piston-like flow

For the segregated flow, thickness of the reservoir considered being $60\ ft$ (larger enough than capillary transition zone) and the reservoir has 5° upward dip angle. To achieve stable front conditions, water is injected at the rate of 100 bbl/day, and the oil viscosity is equal to 1cp. In the unstable interface conditions, water injection rate and oil viscosity are 1000 bbl/day and 3cp respectively. Linear relation between relative permeability and water saturation is considered in the segregated flow ($S_{w_c} = S_{o_r}$ = 0.15,$\acute{k}_{r_w} = 0.5$, $\acute{k}_{r_o} = 0.95$).For the capillary influenced flow, we set $h_{res} = 30ft$. and all the properties are the same as piston-like flow ($\mu_o = 2cp$).

Table 1-Reservoir Properties

Bo	1.3	bbl/stb
Bw	1	bbl/stb
φ	0.18	
Swc	0.2	
Swo	0.2	
K	50	md
μo	05,1,2,5	cp
μw	1	cp
h	10	ft
Width	300	ft
L	2000	ft
Injection rate	500	stb/d
Pin	4500	psi
ρo	45	lb/ft^3
ρw	64	lb/ft^3
Cr	2.00E-06	1/psi
T	150	F
Pb	3000	psi

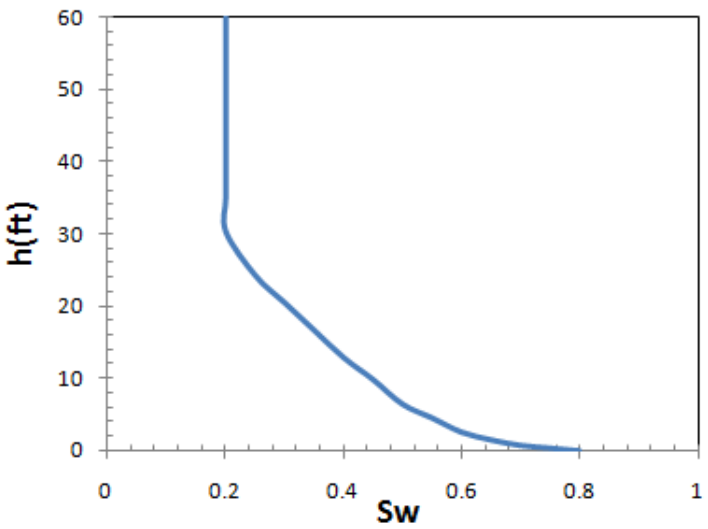

Fig.6-Capillary pressure equivalent height

To introduce simple reservoir heterogeneity, all the mentioned models divided to high permeable zone and low permeable zone. $k = 100\,md$, $\varphi = 22\,\%$ were allocated for high permeable zone and $k = 50\,md$, $\varphi = 18\%$ for low permeable zone. Finally, two-dimensional reservoir including $25 \times 25 \times 1$ grid blocks($80 \times 80 \times 10\,ft$) with different injection patterns was modeled to study radial flow. The properties of the reservoir are the same as piston-like model.

Results:

We considered different values for the oil viscosity ($\mu_o = 0.5\,, 1, 2.5\,cp$) to investigate the effect of different mobility ratios. The results for the case in which oil viscosity is $1\,cp$ are shown in **Fig. 7**.

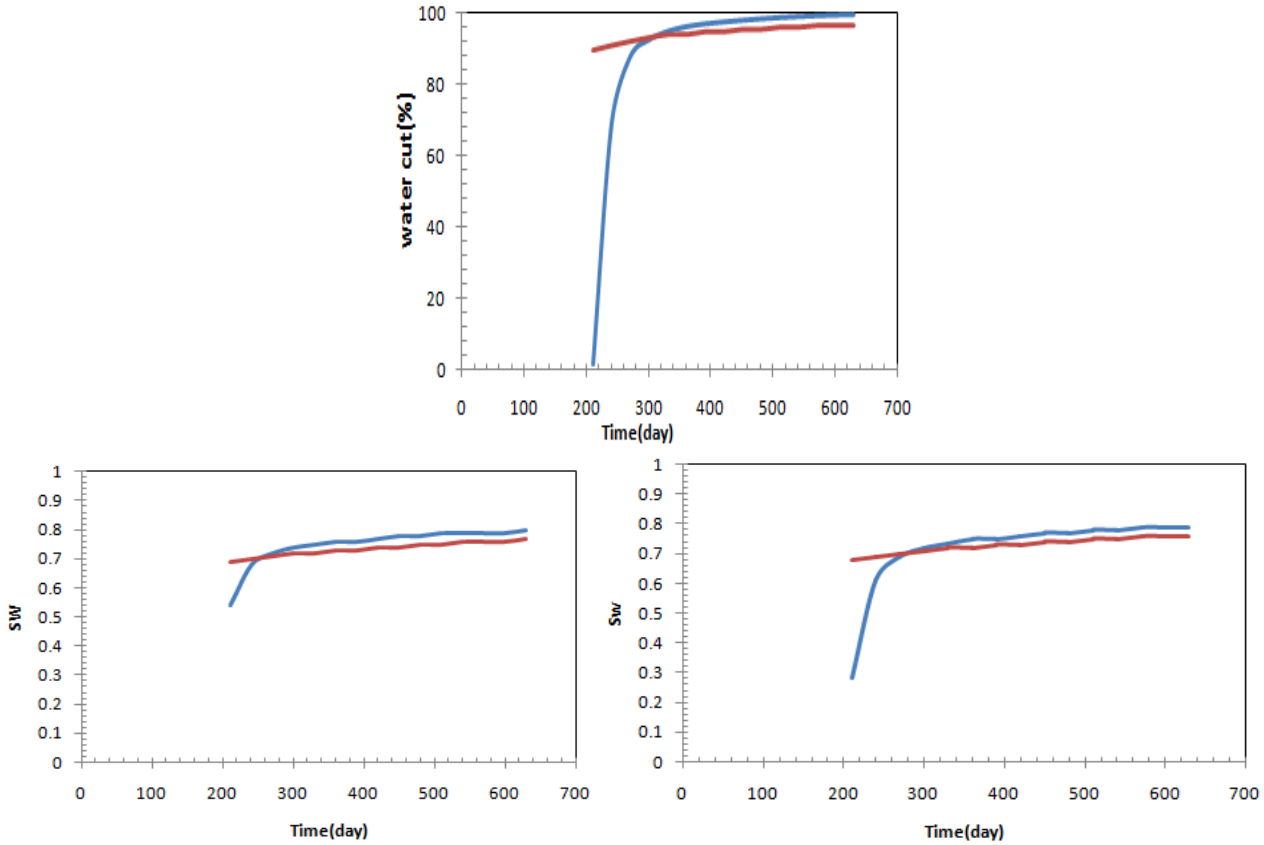

Fig. 7-Water cut match (top) and water saturation profile in the production well grid (bottom left) and 160ft from production well(bottom right,blue → simulation, red→ analytical results)

For this case the breakthrough time (210day) and water cut history results from simulation matched with analytical solutions finding $a = 7350\,, b = -15.85$. Based on water cut history match, analytical results for water saturation are almost the same as simulation results except for early days after water breakthrough(analytical solutions are exact but numerical solutions are approximate). As μ_o increases, S_{wf} and the efficiency of water flooding decrease. Moreover earlier water breakthrough occurs. In this study for oil viscosity equal to 1, 2 and 5 cp it takes almost 600, 1000 and 1800 days respectively to produce all the recoverable oil. Different values for 'a' and "b" parameters were obtained to match the analytical and simulation water cut history for different oil viscosities (**Table 2**).

Table 2-"a"," b", front saturation and breakthrough time in piston-like flow for different μo

μo(cp)	a	b	S_{wf}	tb(day)
0.5	7350	-15.81	0.73	227
1	7350	-15.85	0.68	210
2	7350	-15.8	0.63	190
5	7350	-15.84	0.56	170

For the segregated water displacement $\acute{k}_{r_o}$ and $\acute{k}_{r_w}$ are the parameters that determine the behavior of the analytical solution. When the water front is stable ($G > M - 1; M > 1$) analytical water cut results are more sensitive to $\acute{k}_{r_w}$ and can be matched with simulation results by setting $\acute{k}_{r_w} = 0.45$. This leads to a good match between analytical results and simulation saturation in the production well and the neighboring grids (**Fig. 8**).

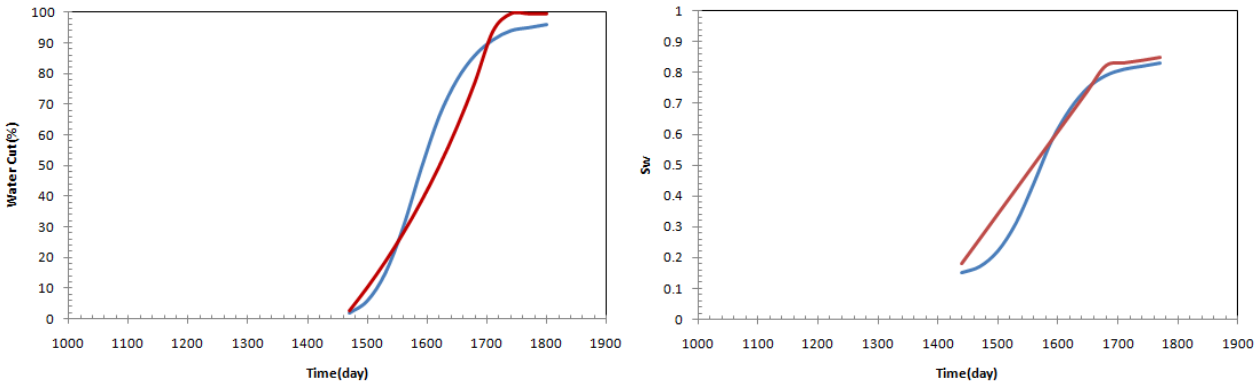

Fig. 8-Water cut match (left) and water saturation profiles for stable interface segregated flow (blue → simulation, red→ analytical results)

When the water front interface is not stable($G < M - 1$), the average difference between analytical and simulation water cut history is minimized at $\acute{k}_{r_o} = 0.9$ and $\acute{k}_{r_w} = 0.5$ (**Fig. 9**). Although the obtained values for endpoint relative permeability minimized the average difference between water cut results, but there is a difference between water cuts (analytical and simulation) just after the water breakthrough. This resulted in a difference in simulation and analytical water saturations (early times) in the well and neighboring grid.

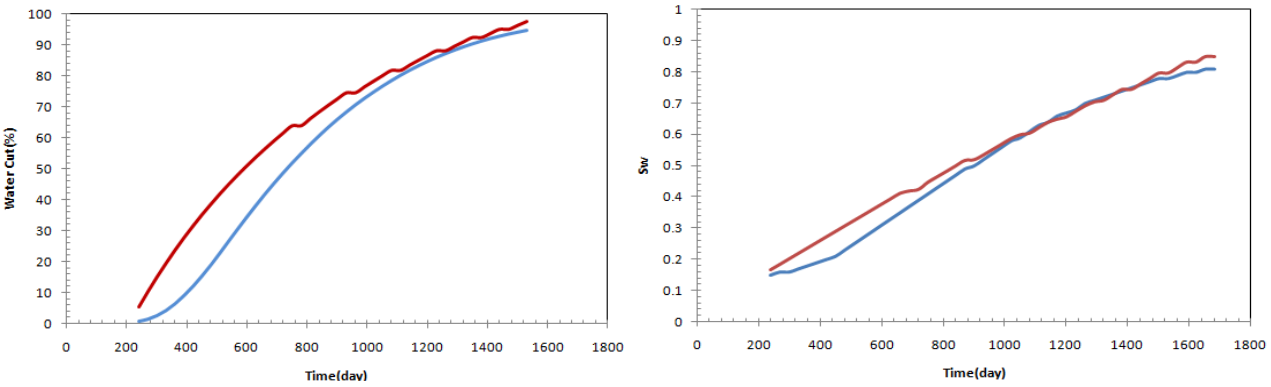

Fig. 9-Water cut match (left) and water saturation profiles for unstable interface segregated flow (blue → simulation, red→ analytical results)

The results of finite capillary transition zone flow ($\mu_o = 2\ cp$) are illustrated in **Fig. 10**. Corey coefficients were obtained ($n_w = n_o$=1.9) to optimize the error function (difference between analytical and simulation) of water cut results. Also relative permeability coefficients (a, b) were determined to minimize the mismatch between water cut results. While both obtained values for set of coefficients minimized the average difference between analytical and simulation water cuts, the analytical water saturation history at the well grid obtained by relative permeability ratio coefficients (a, b) represented better match with simulator saturation results.

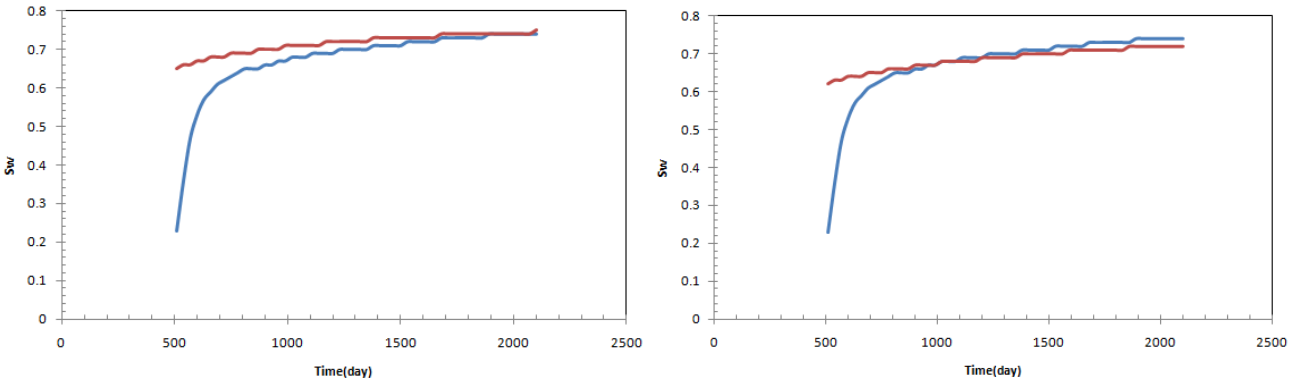

Fig. 10- Comparison between Water saturation profile by Corey coefficients (left) and exponential relative permeability coefficients (right, blue → simulation, red→ analytical results)

Two different cases for heterogeneous reservoirs were modeled based on the placement of the high permeability layer (top and bottom of the reservoir) in favor of all the different flow patterns (piston-like, segregated and capillary influenced). Analytical water cut results were matched with simulation results by finding different relative permeability coefficients. In all the flow patterns, the case that high permeability layer is placed on top of the reservoir demonstrates more accurate results for the analytical water saturation at the well grid (**Fig. 11**).
In the case that high permeability layer is at bottom of the reservoir, gravity and viscous forces act at the same location of the reservoir, resulting in earlier water breakthrough and unfavorable water displacement. When high permeability layer is on top of the reservoir, gravity forces act in the bottom while viscous forces act on the top. The compensation between these two forces makes a favorable and piston-like water displacement, which is a presumption for deriving Buckley-Leverett's formulation. Therefore the analytical water saturation results for the case that high permeability layer is on top of the reservoir is closer to simulation results. The average error (difference between simulation and analytical water saturation) in two different heterogeneous reservoirs for different flow conditions are shown in **Table3**.

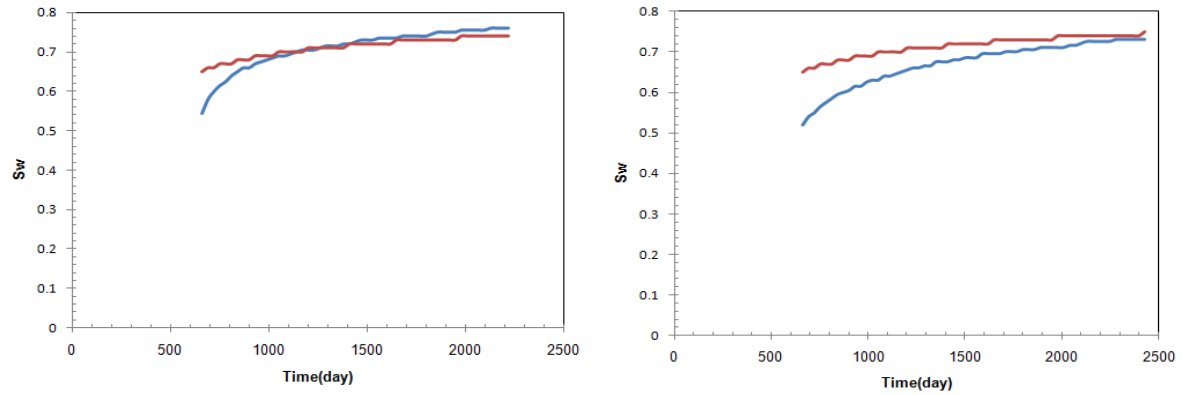

Fig. 11- Water saturation in capillary influenced flow condition when high permeability layer is on the top of reservoir (left) and in the bottom (right, blue → simulation, red→ analytical results)

Table 3-Comparison of water saturation average errors respect to the placement of high permeability layer in the reservoir

High Permeability Layer on Bottom of Reservoir				Average Error (%)	High Permeability Layer on Top of Reservoir				Average Error (%)
Flow condition	Piston-like	μo	2cp	5	Flow condition	Piston-like	μo	2cp	3.5
		a	7200				a	7625	
		b	-17.4				b	-16.4	
		tb	191 day				tb	200 day	
		μo	5cp	3			μo	5cp	1.6
		a	7300				a	7250	
		b	-16.5				b	-16.4	
		tb	169 day				tb	180 day	
	Segregated	μo	3 cp	4		Segregated	μo	3 cp	1.6
		k'_{ro}	0.9				k'_{ro}	0.91	
		k'_{rw}	0.55				k'_{rw}	0.5	
	Capillary Influenced	μo	2 cp	4.5		Capillary Influenced	μo	2 cp	1
		nw	2				nw	1.9	
		no	1.9				no	1.9	

In the two-dimensional water displacement calculations, we consider radial flow of the water front. All the calculations are the same as the Buckley-Leverett's formulations. The only difference is that instead of $X_{S_{wf}}$, we should calculate the radius of S_{wf} as follow:

$$r_{S_{wf}} = \left[\left(\frac{5.615W_i}{\pi h\varphi}\right)\left(\frac{df_w}{dS_w}\right)_{S_{wf}}\right]^{1/2} \qquad (eq.13)$$

Four different well placements (5 spot water injection with production wells in the corner of the reservoir, 5spot water injection with production wells in the middle of the sides, one injection well in the corner and one production well in the front corner, triangular reservoir with injection well in the corner and production well in middle of the front side) are considered for water injection and the same procedure were applied to determine analytical water saturation in the vicinity of the production well(**Fig. 12**).

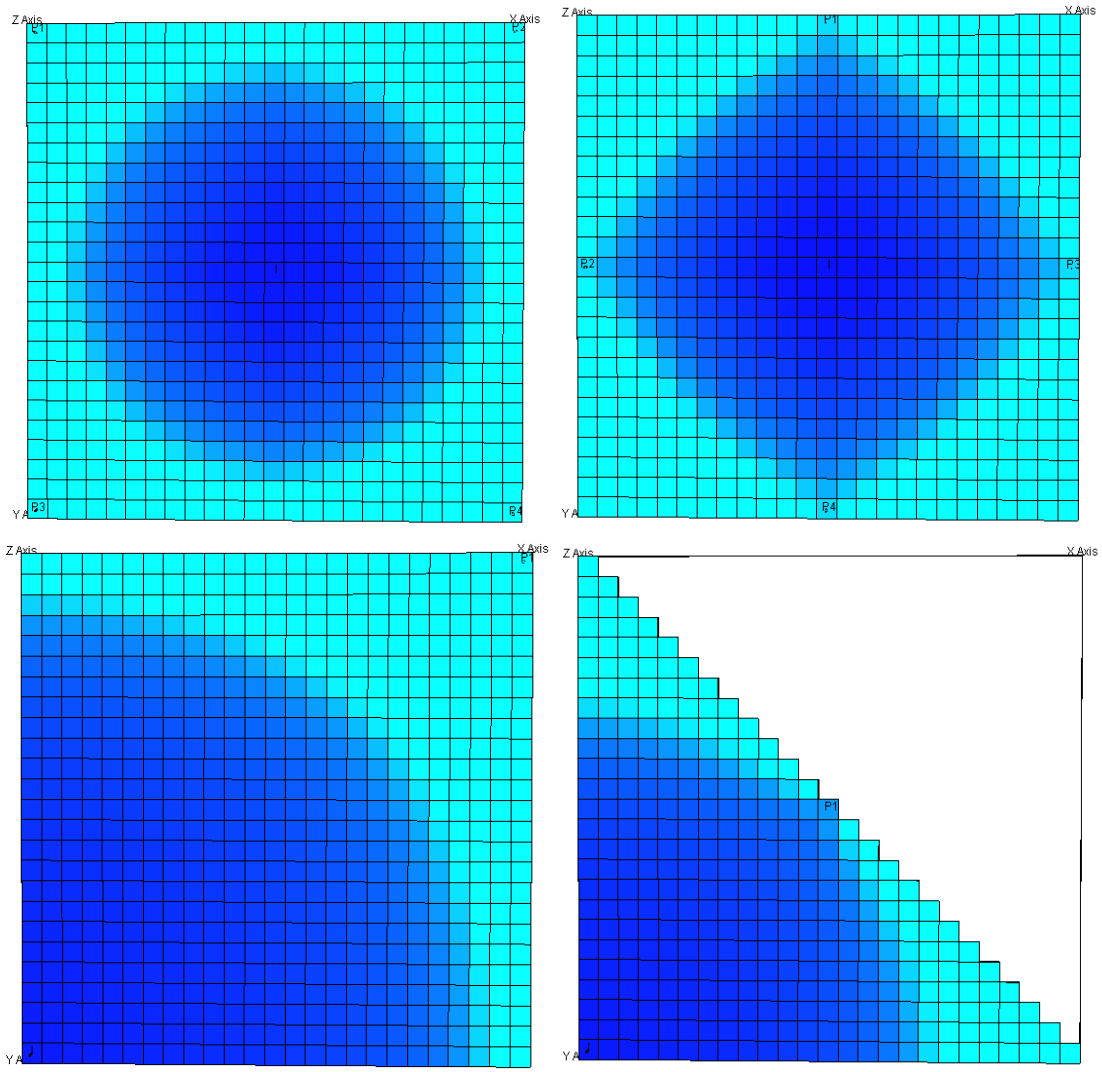

Fig.12- Different well placement for 2D water displacement in the reservoir,5 spot(top left),5 spot with the production wells in the middle of the sides(top right), two wells in the corners(bottom left) and 2 wells in triangle shape reservoir(bottom right)

In all of these models analytical water cuts were matched with the simulation results. Among them the saturation profile in the well grid for the last well placement (triangular shape reservoir) represents the least deviation from the simulation results. (**Fig. 13**)

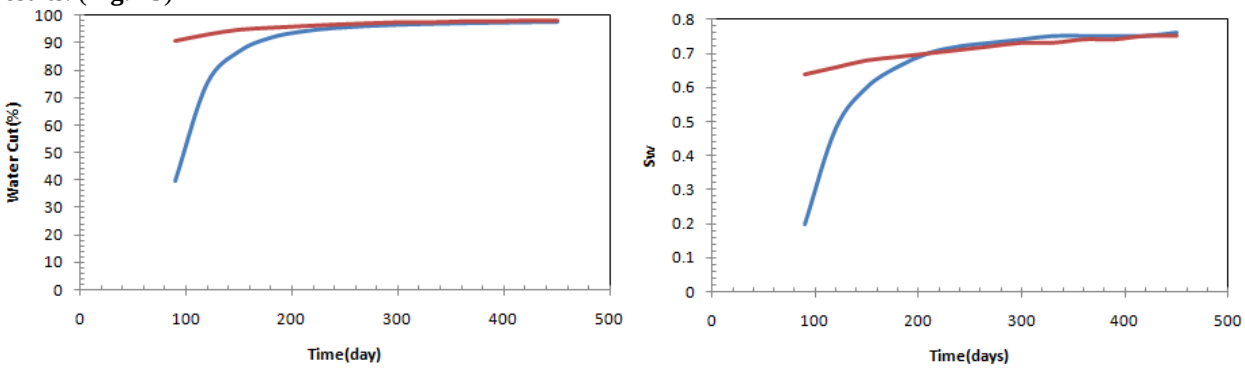

Fig. 13-Water cut match (left) and water saturation profiles for radial flow in triangle shape reservoir (blue → simulation, red→ analytical results))

Conclusion:

We have investigated the efficacy of analytical solutions in determination of reservoir fluid saturation distribution based on the production data. Analytical models are not computationally expensive compare with reservoir simulation but they can not be implemented in coplex problems.

-Three representations for relative permeability were used in analytical models to match water cut results in different flow conditions. Exponential form of relative permeability ratios ($^{K_{ro}}/_{K_{rw}} = ae^{bS_w}$) provided accurate results for saturation distribution in the reservoir for piston-like and capillary influenced flow conditions. In segregated flow, end point relative permeability was used to generate water cut results. For the case that water front interface is not stable, analytical model can not generate an accurate match with simulation water results at the early time after water breakthrough.

-Two layered 1_D heterogeneous reservoir water displacement studied under 3 different flow conditions. More precise results for water saturation profiles were achieved in the reservoirs with high permeability layer on the top.

-The Buckley_leverett's formulations for radial flow (2D) were applied for different injection patterns. The best match between analytical and simulation water saturation results was observed for the case with one injection-one production well in the triangular shape reservoir

Nomenclature

a = intercept of $\frac{K_{ro}}{K_{rw}}$ vs. Sw
A = Area, ft^2
b = slope of $\frac{K_{ro}}{K_{rw}}$ vs. Sw
bf = water front fractional thickness
Bo = oil formation volume factor, bbl/stb
Bw = water formation volume factor, bbl/stb
Cr = formation compressibility factor, 1/psi
fw = fractional water cut @ reservoir condition
fwf = fractional water cut @ Swf
fws = fractional water cut @ surface condion
G = gravity number
h = reservoir thickness, ft
K = absulote permeability, md
Kro = oil relative permeability
Krw = water relative permeability
$K'ro$ = end point oil relative permeability
$K'rw$ = end point water relative permeability
L = reservoir length, ft
M = end point mobility ratio
n_w = Corey exponent for water relative permeability
n_o = Corey exponent for oil relative permeability
Pb = bubble point pressure, psi
Pin = reservoir initial pressure, psi
q_o = oil flow rate, bbl/day
q_w = water flow rate, bbl/day
q_t = total flow rate, bbl/day
r_{swf} = radius of front saturation, ft
T = tempreture, F
Sw = water saturation
Swc = connate water saturation
Swf = front water saturation
$Swor$ = irreducible oil saturation
V = fluid velocity, ft/sec
Wi = cumulative water injection,bbl
X = distance, ft
Xbf = distance of water front fractional thickness, ft
Xs_{wf} = distance of front water saturation, ft

β = angle between fluids interface and the direction of flow, rad
φ = porosity, %
ρo = oil density, lb/ft^3
ρw = water density, lb/ft^3
θ = reservoir angel, rad
μ_o = oil viscosity, cp
μ_w = water viscosity, cp

References

1. Ahmed, T, 2002, Reservoir Engineering Handbook, Second Edition, Elsevier

2. Bruning, H, 2002, Multiphase Flow in Porous Media, Delft University, Netherlands

3. Dake, L.P, 2001, The Practice of Reservoir Engineering (Revised Edition), Elsevier

4. Dake, L.P, 1983, Fundamentals of Reservoir Engineering, Elsevier

5. Dietrich, J.K, Little, J.E, 1975, A Method for Determining Reservoir Fluid Saturations Using Field Production Data, SPE Journal, Volume 15. Number 6, SPE-3961-PA

6. Ershaghi, I, Omorigie, O, 1978, A Method for Extrapolation of Cut vs Recovery Curves, Journal of Petroleum Technology, Volume 30, Number 2,SPE-6977-PA

7. Kulkarni, K.N, Datta-Gupta, A, 2000, Estimating Relative Permeability From Production Data: A Streamline Approach, SPE Journal, Volume 5, Number 4, SPE-66907-PA

8. Mohaghegh, S.D, Modavi, A, Hafez, H, Haajizadeh, M, Kenawy, M, Guruswamy, S,2006, Development of Surrogate Reservoir Models (SRM) For Fast Track Analysis of Complex Reservoirs, Intelligent Energy Conference and Exhibition, 11-13 April 2006, Amsterdam, The Netherlands,SPE-99667-MS

9. Sitoru , J, Sofyan, A, Abdulfatah, M.Y,2006, Developing A Fractional Flow Curve from Historic Production to Predict Performance of New Horizontal Wells, Bekasap Field, Indonesia, PE Asia Pacific Oil & Gas Conference and Exhibition, 11-13 September 2006, Adelaide, Australia,SPE-101144-MS

10. Weber, D, Edgar, F.E, Lake, L.W, Lasdon, L,Kawas, S, Sayarpour, M,2009, Improvements in Capacitance-Resistive Modeling and Optimization of Large Scale Reservoirs, SPE Western Regional Meeting, 24-26 March 2009, San Jose, California,SPE-121299-MS